25th ABCM International Congress of Mechanical Engineering
October 20-25, 2019, Uberlândia, MG, Brazil

COB-2019-0173
THERMAL ANALYSIS DURING AGING OF A LITHIUM-ION CELL USING A MODIFIED DIFFERENTIAL VOLTAGE TECHNIQUE

Luis Artur Ricardo Françoso
Santiago del Rio Oliveira
Rodolfo Castanho Fernandes
São Paulo State University (UNESP), School of Engineering, Bauru
arturfrancoso@yahoo.com.br
santiago.oliveira@unesp.br
rodolfocf@ieee.org

Abstract. *The study of thermal performance of battery cells is extremely important once it directly impacts on user safety. This paper aims to analyze the thermal behavior of a cylindrical lithium-ion cell $LiFePO_4$ 8000 mAh, 38120 size to better understand the effect of aging due to repetitive charge-discharge cycling on the surface temperature and thus estimate the internal temperature using an iterative method named differential voltage technique. Comparing the literature, the present paper adds some improvements such as the inclusion of radiation and the use of an internal resistance as a function of cycle number obtained experimentally, in addition to proposing a comparison of two alternatives for calculating the generated heat: the first, only with the effect of reversible heat and the second one omitting reversible heat term. Under the experiment conditions, the cell was placed at ambient temperature of 308 K and at a discharge C-rate of 2C. After 600 cycles under these conditions, it was possible to verify the effects of aging through the decrease of ohmic resistance and increase in the cell temperature after the discharge phase.*

Keywords: *thermal behavior, lithium-ion cell, differential voltage technique, aging effects.*

1. INTRODUCTION

When analyzing the global scenario in which the energy crisis is a widely addressed issue, especially when it comes to sources from oil, alternative sources of energy tend to become more common in our society. Energy accumulators such as supercapacitors and lithium-ion cells, whose main advantages are high specific energy and power, in addition to long lifetime, appear as suitable alternatives for energy storage, be it wind or solar energy.

As for lithium-ion cells, as discussed by Nazari and Farhad (2017), their good cyclic performance, low self-discharge rate, lack of memory effect and availability to operate at high voltages make these energy storage devices suitable for many applications, such as power tools and electric vehicles and large-scale grid storage sytems. However, not so advantageous properties are still present in lithium-ion cell and, according to Dong *et al.* (2018), this type of cell is vulnerable to overheating when subjected to high charging or discharging rates. Operations at low temperatures also cause problems related to autonomy and performance, as highlighted by Tripathy *et al.* (2017). In this context, understanding the thermal behavior of the cell is relevant for the design of, for example, cell heating and cooling systems. When multiple cells are put together to form high capacity batteries (large number of cells associated), safety concerns scale-up, so that thermal behavior and analysis are not only necessary but mandatory.

To evaluate the harmful effects of high temperatures and also to understand the internal electrochemical processes of the cell for its management, it is indispensable to understand about its internal temperature. In this sense, Shuai *et al.* (2017) describe two ways of obtaining an approximation of the internal temperature, through contact and contactless measurement. In contact measurement, sensors such as thermocouples are inserted in the cell core to monitor the internal temperature. This is a difficult task, prone to failure and cannot be applied to all cell shapes. In contactless measurement, without sensor insertion, the internal temperature can be obtained through computational simulation (such as finite elements method) or through electrochemical impedance spectroscopy. This last option is a complex method, based on expensive scientific apparatus.

A simpler method, in comparison with the two mentioned measurements, was proposed by Tripathy *et al*. (2017). This method, known as differential voltage technique, aims to estimate the internal temperature of the cell by relating Ohm's law to the first law of thermodynamics to calculate the effective electrical resistance of the cell under different conditions of ambient temperature and discharge rate. The objective of the present study is to analyze the thermal behavior of a lithium-ion cell, according to Fig.1, during the charge/discharge cycles, to evaluate the effects of its aging through temperature variation on its surface and, thus estimate the internal temperature with sufficient accuracy. In this

case, "sufficient accuracy" means accuracy enough to allow prediction of temperature rise inside the cell, under certain discharge condition, so that the information can be used to design a battery pack or to compare the cell with other existing cells or to check if there is any chance of reaching maximum cell temperature (as indicated in the cell datasheets). The differential voltage technique was chosen as this study considers this technique presents good agreement with experimental results.

Figure 1. Lithium-ion cell sample.

The contributions of the present study are: a) improvements in the differential voltage technique, such as obtaining an internal electrical resistance through discharge pulse test for each one hundred cycle, b) defining internal electrical resistance as a function of charge/discharge cycles, c) determination of the average value of the convection heat transfer coefficient using an appropriate correlation, d) inclusion of a heat rate dissipated through thermal radiation and e) inclusion of the reversible heat in the heat rate generation, based on Bernardi's equation. In addition, to calculate the internal temperature of the cell, two different models were used to determine the heat rate generated inside the cell. A comparison of the results for the internal temperature was also carried out. The first model is the one used in this study based on Bernardi's equation, which includes a term based on a reversible heat source in the heat rate generation. The second model the reversible heat rate is omitted, remaining only irreversible heat source. Forgez *et al.* (2010) also used these two models for the thermal analysis of a cylindrical cell.

2. EXPERIMENTAL PROCEDURE

2.1. Procedure

The experimental procedure was performed from a lithium-ion cell Headway 38120HP, composition of the positive electrode $LiFePO_4$, cylindrical geometry and 8000 mAh capacity, 3.2 V. Table 1 shows the properties of the lithium-ion cell from the cell's datasheet.

Table 1. $LiFePO_4$ cell specification

CELL CHARACTERISTICS		
Nominal capacity		8000 mAh (0.5C)
Nominal voltage		3.2 V
Cell internal resistance		≤ 5 mΩ
Maximum charge current		5C (40 A)
Maximum charge voltage		3.65 ± 0.05 V
Maximum continuous discharge current		20C (160 A)
Maximum discharge current		25C (200 A)
Cut-off discharge voltage		2.0 V
Maximum dimensions size	Diameter	38 ± 1 mm
	Height	132 ± 1 mm
Mass		335 g

The following equipment were used: a thermal chamber with temperature control, a programmable charge/discharge cell test manager Cadex C8000, which also stores the information in each run cycle, K-type thermocouple attached in the middle of the lateral external surface and an uninterruptible power supply (UPS) to protect the experiment from possible power outages in the network. Fig. 2 shows the experiment setup:

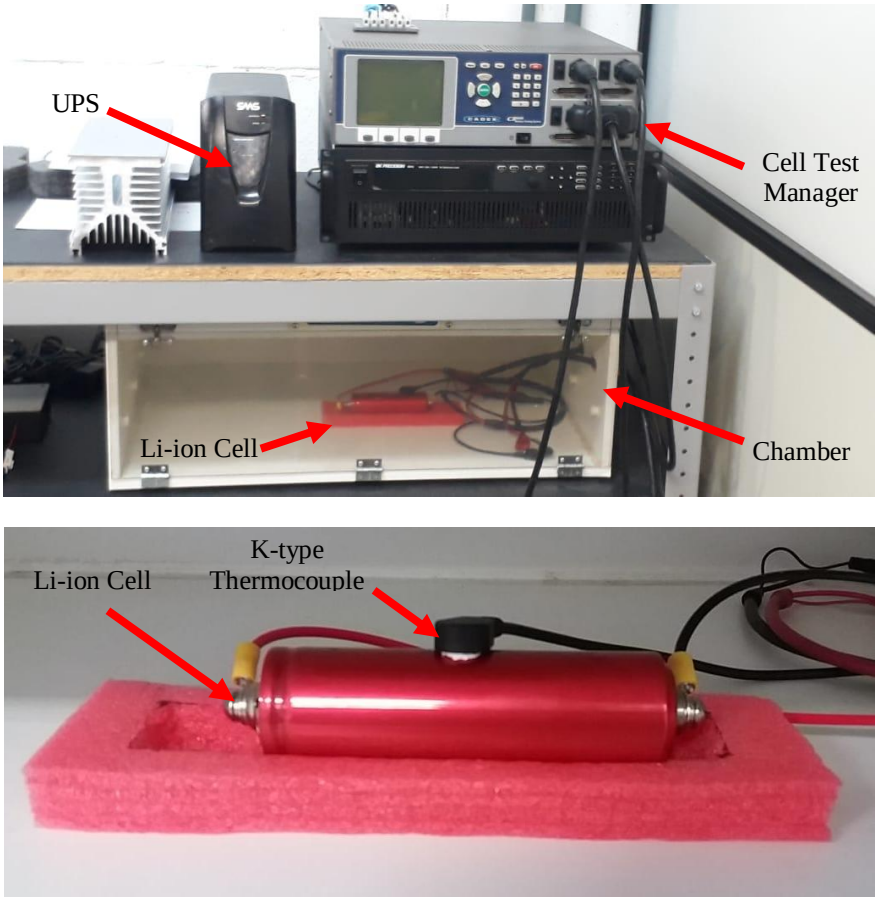

Figure 2. Experimental setup equipment above and below, details of the thermocouple positioning in the cell.

At first, the completion of the experiment was established to occur when the cell discharge capacity reached 30% of the initial capacity. This would correspond to a large number of cycles, probably over 1000 cycles. However, during the execution of the experiment it was verified that the time needed to reach a discharge of 30% would be long and considering that the place used for the experiment could not meet this deadline, the investigators decided to reduce it, thus presenting partial results for analysis. Thus, 600 charge/discharge cycles were performed, with data collection performed every 100 cycles.

At each cycle, the cell used in the experiment was charged at a C-rate of 0.5C (4 A) and discharged at a C-rate of 2C (16 A), at a total of approximately 2.5 hours per cycle, (2 hours for charging, 0.5 hours discharging, typically), which enabled an average of 8 to 10 cycles per day of experiment. Such protocol complies with the safety determinations by the cell manufacturer for executing their processes, both for charging and discharging. The limiting parameters of charge and discharge voltages established for the experiment were 3.55 V and 2.0 V (safety cut-off to avoid damage). The procedure was initiated with the placement of the cell inside the thermal chamber, horizontally. The cell was connected to the cell test manager and then a working temperature of 308.15 K was maintained. The test was started, and the values were automatically recorded to the memory of the charge/discharge test manager. Data collection was performed every 100 cycles (approximately 10 days). During the data collection event, charging and discharging cycles were logged at 1 second sampling rate (in other words, voltage and current data points logged every 1 second). The equipment used in the experiment remained constantly connected to a UPS to ensure no interferences such as electrical faults or voltage surges.

2.2. Determination of the internal temperature of the cell

For estimating the internal temperature of the cell in relation to time, an iterative sequence of the following equations was used according to the differential voltage technique. With the 2C discharge rate, the iterative procedure was carried out 1800 times, referring to 1800 seconds (30 minutes) of the discharge phase. In this technique, the generated heat rate is calculated considering the irreversible and the reversible heat sources. The estimation is performed through the iterative method for each second of the discharge stage. The initial conditions of the iterative method are: at the initial time $T_{in}(t=0) = T_S = T_\infty = T_{sur}$ and that $q_{cond}(t=0) = 0$, where T_∞ is the ambient temperature, T_{sur} is the temperature of the surroundings and q_{cond} is the heat transfer rate by conduction. Other

properties used in the mathematical modeling: heat transfer area (*A*), cell length (*L)*, external radius (r_s), internal radius (r_i), cell mass (*m*), cell electrical resistance (*R*), thermal conductivity of cell (*k*), cell specific heat (*c)*, average value of the convection heat transfer coefficient based on the external diameter of the cell ($\bar{h}_D$), the cell surface emissivity (ε), the Stefan-Boltzmann constant (σ), voltage (*U*), the electrical current (*I*), q_{conv} is the heat transfer rate by convection, q_{rad} is the heat transfer rate by radiation and *(ΔT*) is the increase in internal temperature every second.

The heat transfer area was calculated using the external radius of the cell and its length, obtained from the datasheet of the cell. The cell mass was also obtained from the datasheet of the cell and considered the internal radius of the cell spiral as 0.01 m. The electrical resistance R_0, which varies with each cycle, obtained through the pulse test, will be detailed in section 2.3. Regarding the specific heat and the cell thermal conductivity, these properties depend on the cell characteristics. The weighted average of the values of specific heat and thermal conductivity related to the thickness (*e*) and each cell layer were used, as according to Wang *et al.* (2017). The thicknesses of each layer were the same ones adopted by Nadimpalli and Abraham (2015) for a cylindrical cell model 18650. Therefore:

$$c = \frac{\sum_i c_i e_i}{\sum_i e_i} \tag{1}$$

$$k = \frac{\sum_i k_i e_i}{\sum_i e_i} \tag{2}$$

Here, *i* denotes each of the cell layers, which repeat themselves in a spiral. To facilitate calculations, the cell was assumed to be an isotropic material. In the upper internal part of the chamber there is a ventilation system directed on the cell lying horizontally at a height of 0.22 m so that air flows at a velocity of 0.5 m/s. For the calculation of the average value of the convection heat transfer coefficient, $\bar{h}_D$ based on the external diameter (*D*) of the cell, the ambient air properties (dynamic viscosity, specific mass and thermal conductivity, (k_{ar})) were determined at the temperature of 308.15 K through polynomial expressions presented by Zografos *et al*. (1986). From these properties, the numbers of Rayleigh (Ra_D), Prandtl (Pr), Grashof (Gr_D) and Reynolds (Re_D) were calculated. The possibility of mixed convection was initially admitted but was later discarded due to an analysis of heat transfer processes by forced convection and natural convection. It was found that natural convection can be neglected in relation to forced convection in the physical situation under analysis. In this context, an estimate of the mean coefficient of heat transfer can be made using the Churchill-Bernstein (1977) correlate proposed, valid for cross-flow on long horizontal cylinders, according to Eq. (3):

$$\bar{h}_D(t) = \frac{k_{ar}(t)}{D}\left\{0.3 + \frac{0.62\,\mathrm{Re}_D(t)^{1/2}\,\mathrm{Pr}(t)^{1/3}}{[1+(0.4/\mathrm{Pr}(t))^{2/3}]^{1/4}}\left[1+\left(\frac{\mathrm{Re}_D(t)}{282.000}\right)^{5/8}\right]^{4/5}\right\} \tag{3}$$

To calculate the heat transfer rate by thermal radiation between the cell and the walls of the chamber, the simplified radiation model was used according to Bergman *et al.* (2014). The study considered the material of the cell can as stainless steel, which is typically used for that purpose. So that ε = 0.2. The cell's label and its effects on the emissivity were disregarded. Also, it was considered that the walls of the thermal chamber were also at constant temperature of 308.15 K. Considering the first proposal for the heat generated rate inside the cell (q_{g1}) the following calculation procedure was performed according Eqs. (4) to (10):

$$R(t) = \frac{U(t-1) - U(t)}{I} + R_0 \tag{4}$$

$$q_{g1}(t) = R(t)I^2(t) + I(t)T_S(t)\frac{dU}{dT} \tag{5}$$

$$q_{conv}(t) = \bar{h}_D(t)A[T_S(t) - T_\infty] \tag{6}$$

$$q_{rad}(t) = \varepsilon\sigma A[T_S^4(t) - T_{sur}^4] \tag{7}$$

$$\Delta T(t) = \frac{[q_{g1}(t) - q_{cond}(t) - q_{conv}(t) - q_{rad}(t)]}{mc} \tag{8}$$

$$T_{in}(t) = T_{in}(t-1) + \Delta T(t) \tag{9}$$

$$q_{cond}(t+1) = -\frac{2\pi kL[T_{in}(t) - T_S(t)]}{\ln(r_s - r_{in})} \tag{10}$$

As the method used by Tripathy *et al*. (2017), in which the electric resistance of the cell is calculated by dividing ΔU by I, added to internal electric resistance. This electric resistance is obtained by the pulse test proposed by the USABC test procedure manual (1996), an analogy of the cell with an electric circuit is made. Although the USABC procedure uses an R circuit, an RC circuit was used in this investigation. This allows simplifying the real complexity of the electrochemical processes involved in the cell using a circuit model that approximates the effects produced by these phenomena. In this way it is possible to determine the ohmic electrical resistance (R_0), the electric resistance of charge transfer (R_1) and the capacitance of the metal-electrolyte interface (C).

2.3. Determination of the ohmic resistance R_0 by the pulse test

To perform the iterative procedure described above, it is necessary to obtain the internal electrical resistance R_0. Therefore, pulse test was performed before the beginning of the cycles and afterwards, the same test every 100 cycles. The test procedure consisted in placing the cell at the temperature of 308.15 K, allowing it to stabilize at that temperature for at least 4 hours. The cell was charged with an arbitrarily chosen C-rate of 0.5 C, with the following safety values being set at 3.55 V for maximum voltage and 0.4 A for the cut-off current. Next, the cell was allowed to stand for 1 hour before a square waveform discharge pulse was applied. After the discharge pulse was applied, the voltage slowly increases, but no longer reaches its initial value due to the suffered discharge. The value of the voltage variation between the end of the pulse and the first voltage value after removal of the charge is defined as ΔU_0, while the value of the voltage variation of the end of the pulse to the steady state voltage as ΔU_∞. The stabilization time for the steady state can be calculated from Fig. 3 as well as parameters R_0, R_1 and C.

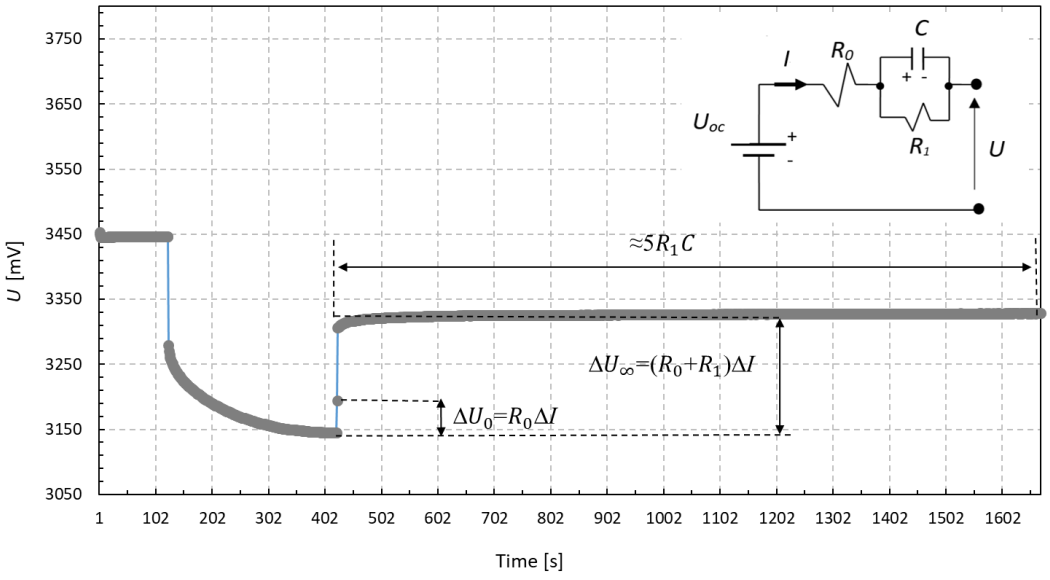

Figure 3. Pulse test performed every 100 cycles.

The U_{oc} in the Fig. 3 means open circuit voltage. The resistance R_0 can be determined by Eq. (11):

$$R_0 = \frac{\Delta U_0}{\Delta I} \tag{11}$$

2.4. Bernardi's model for calculating heat transfer rate

The model presented by Bernardi *et al*. (1985) to calculate the heat generation rate (q_g) was also used in this paper to complement the differential voltage technique. In this model, a reversible portion of heat is included. According to Eq. (5), the first term on the right refers to the heat generation rate by the resistive dissipation, and the second term refers to the reversible heat rate from the entropy variation of the cell reaction, with dU/dT as the entropy coefficient which varies with temperature and the state of charge (*SoC*).

The calculation of q_{g1} was carried out only for a *SoC* = 0% (condition of total discharge). It was obtained experimentally after the total discharge of the cell, by the cell manager. The cell was placed under four different ambient temperature conditions (273 K, 294 K, 303 K and 323 K) and was kept for approximately 2 hours in each condition so that temperature was stabilized inside the cell. Thus, for each temperature a cell open-circuit voltage value was measured. All of these data were stored in a data logger Graphtec GL220 at a 1 sample/second rate. The experimental setup can be seen in Fig. 4, for room temperature measurement.

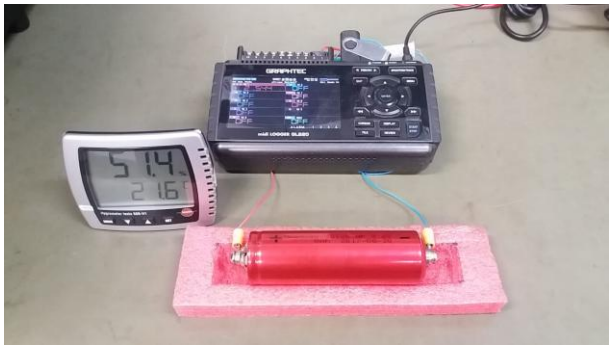

Figure 4. Experimental setup to obtain the entropy coefficient.

3. RESULTS AND DISCUSSIONS

Results obtained for ΔU_0, ΔU_∞, R_0, R_1 and C for the 600 cycles using the pulse test can be seen in Tab. 2:

Table 2. Pulse test results

Cycle number	0	100	200	300	400	500	600
ΔU_0 (V)	0.081	0.161	0.159	0.154	0.150	0.149	0.145
ΔU_∞ (V)	0.174	0.184	0.181	0.174	0.170	0.167	0.163
R_0 (mΩ)	20.25	40.25	39.75	38.50	37.50	37.25	36.25
R_1 (mΩ)	23.25	5.75	5.50	5.00	5.00	4.50	4.50
C (kF)	5.15	43.30	51.49	58.24	71.04	32.27	79.96

The *RC* circuit used in this experiment is a better approximation of the equivalent circuit for a cell than the simple *R* circuit. From the results in Tab. 2, this study affirms that R_0 represents a very good approximation of the internal electric resistance for each cycle, except for the initial cycle, where $R_0 \approx R_1$. Therefore, the choice for R_0 was reasonable to estimate the generated heat rate of the cell. Equations (1) and (2) allowed to obtain the values 1209 J/(kg.K) and 0.892 W/(m.K), respectively, adopted as constants throughout the experiment. The average value of the convection heat transfer coefficient, on the other hand, varied little throughout the experiment. The charge/discharge cell test manager allowed to obtain the surface temperature of the cell throughout the experiment, given the importance of evaluating the behavior of the cell and estimating its own internal temperature. In addition, the results of temperatures that were analyzed and compared refer only to the end of the discharge process.

Experimental results of the test to obtain the entropy coefficient can be visualized in Fig. 5. According to Samba (2015) and Wang (2016), the behavior of the variation between voltage and temperature is typically linear. Using a linear regression, -0.124 mV/K for the entropy coefficient for a fully discharged cell was obtained.

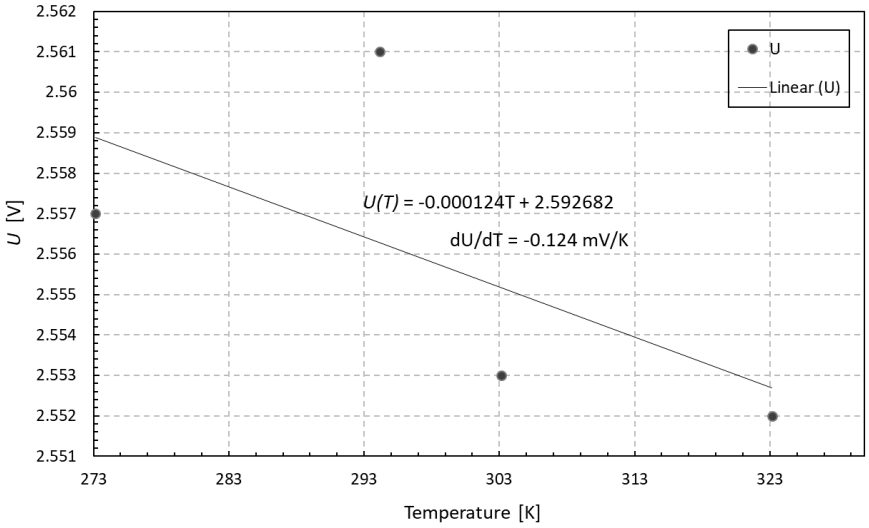

Figure 5. Entropy coefficient with *SoC*= 0%.

The T_{sur} values were collected every second by the cell test manager and subsequently passed through a filter, and its value at the end of the discharge for the initial cycle and the cycles of numbers 100, 200, 300 and 400, was 313.2 K. For the cycles of numbers 500 and 600 there was a slight increase, reaching 313.6 K. It is noteworthy that during the charge process a C-rate of 0.5 C was used, which allowed the cell temperature to return to the ambient temperature of 308.15 K before the following discharge. After the use of the modified differential voltage technique to obtain the internal cell temperature, the following values were obtained: in the initial cycle, 320.2 K; for the 100th cycle 329.1 K; for the 200th cycle 328.6 K; for the 300th cycle 328.0 K; for the 400th cycle 327.5 K; for the 500th cycle 327.3 K and for the 600th cycle 326.8 K. These results can be seen in Fig. 6.

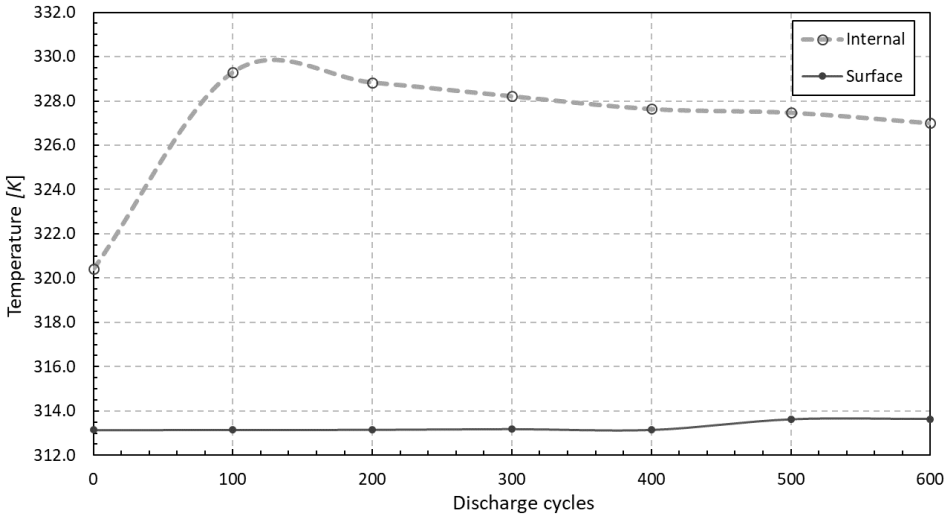

Figure 6. Comparison between T_S and T_{in} for a discharge in 2 C.

The estimation of the internal temperature of the cell through the modified differential voltage technique presented results compatible with the experiment by Waldmann *et al.* (2015), which, for a same cell format and the same C-rate obtained a maximum variation in the internal temperature of 8 K, and in this work an average value of 14 K was obtained. However, one must consider the fact that the chemical compositions of the cells are different, and also possible considerations for the transference portion by conduction, as well as for obtaining the internal electrical resistance.

When analyzing the results obtained for R_0, in Tab. 2 and heat transfer rates in Fig. 7, a decrease of the values as the cycles of cell use increases is observed. This decrease is related to the reduction of the charge capacity (C_c), which

the cell suffers with aging. Values for C_c after the discharge cycles can be calculated by summing the cell charge at each time *t* by the expression $C_c = \sum I\Delta t$, as seen in Tab. 3:

Table 3. Capacity charge per cycle.

Cycles number	0	100	200	300	400	500	600
C_c (Ah)	8.3122	8.0840	7.9100	7.8156	7.8053	7.7301	7.6805
% of Initial C_c	100	97.3	95.2	94.0	93.9	93.0	92.4

From Fig. 7, it is verified that the cell dissipated heat by conduction represents the largest portion of the dissipated heat rate, over 50% of the heat rate generated inside the cell. However, the convection heat and radiation rates represent a very low portion of the dissipated heat rate, approximately 2% of the heat rate generated inside the cell**.** The remaining heat, not dissipated is the portion responsible for the increased internal temperature.

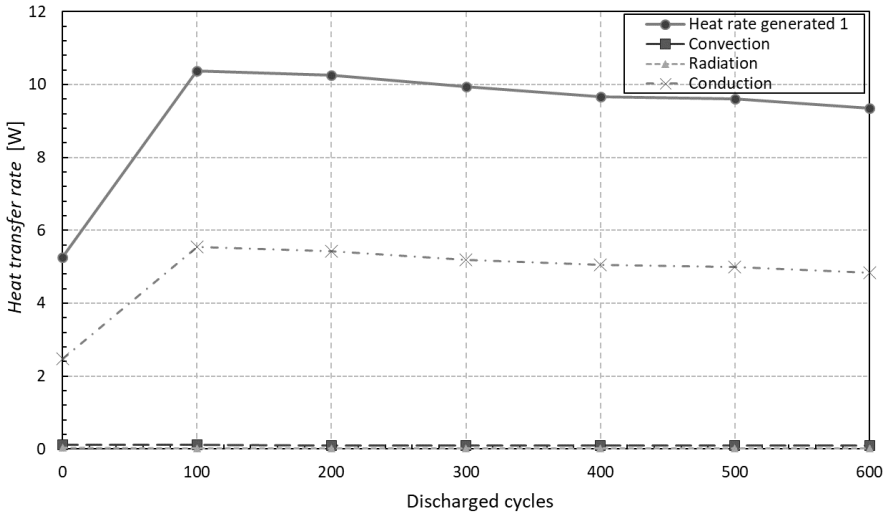

Figure 7. Quantification of the generated heat rate from the ohmic portion, and their respective dissipation portion.

Comparing the two models for obtaining the heat generated rate q_{g1}, which considered the reversible source and q_{g2}, which omitted this heat source, Fig. 8 shows a very small variation in the estimate of the internal temperature of the cell. An increase of approximately 0.2 K was observed between the internal temperatures obtained by the first proposal, not reaching 2% in the participation of the estimate internal temperature.

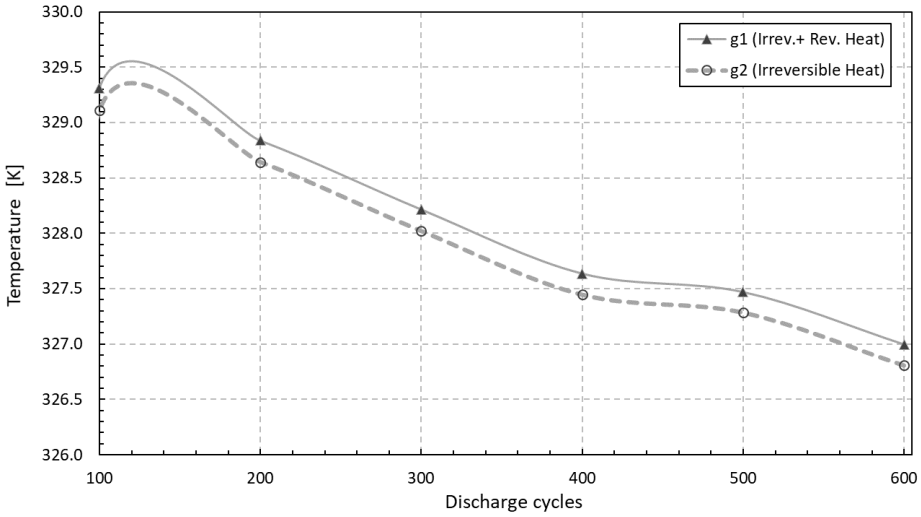

Figure 8. Comparison between internal temperatures using q_{g1} and q_{g2}.

A comparing between the heat portions in the generated heat rate is showed in the Fig. 9 for the initial cycle and the 600th cycle. This graph shows that the generated heat originated from ohmic electrical resistance is more relevant than others sources. And even as this electrical resistance decreases over the cycles, its portion of contribution remains predominant.

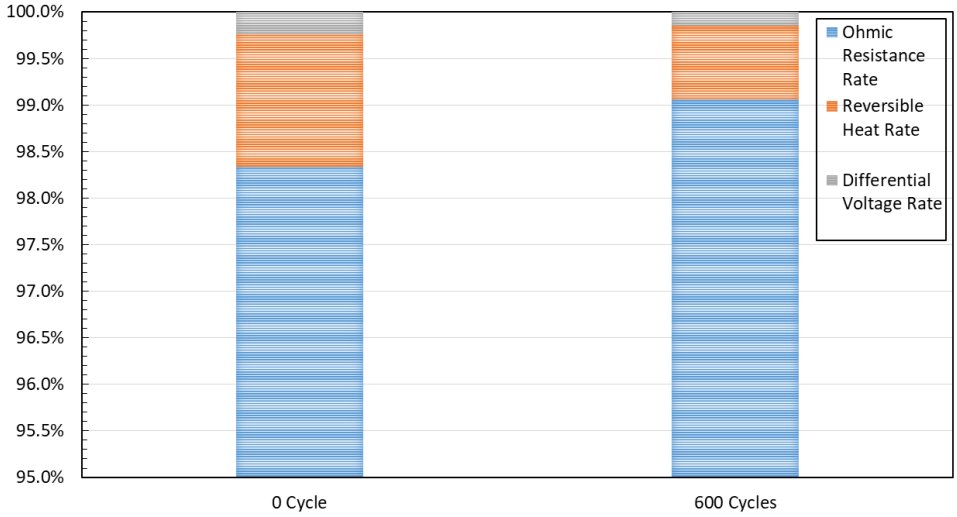

Figure 9. Generated heat rate portion.

Finally, using the proposed model for internal temperature estimation, which adds the five improvements mentioned in the introduction, compared with the differential voltage technique applied to a cylindrical cell, there was a great difference, except for the first cycle due exclusively to the correction for each cycle of the value of R_0 used in the proposed model since in the differential voltage technique the same initial value of R_0 was considered. The other improvements added as the radiation factor in the dissipated heat and the reversible source of heat generation had a small contribution as seen in the values presented in the initial cycle.

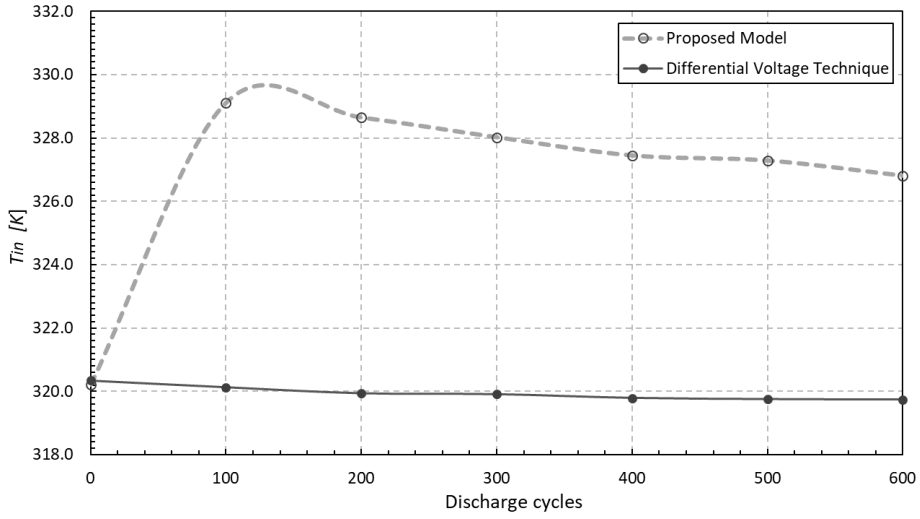

Figure 10. Comparison between proposed model and differential voltage technique.

4. CONCLUSIONS

After the experiment, it was observed that the cell aging brought a reduction of the cell capacity, as expected, and also a reduction in the internal electrical resistance, evidenced by the ohmic resistance portion R_0, which directly influenced the heat generation rate. Although the experiment was terminated earlier than expected, a slight variation in cell surface temperature was noted during the cell aging course, especially in the initial cycles. Initially the internal temperature is in the order of 320 K (new cell, zero cycles) but may reach up to 330 K at the 100th cycle. This important

result has practical relevance since it indicates that cell internal temperature rapidly changes in the first cycles of the cell life. This initial temperature increase may be a concern in batteries, where the heat generation of each cell is summed up and can lead to over temperature issues and calibration errors at the battery monitoring system, if this behavior is not properly accounted for. It is also important to notice from Fig. 7 that generated heat doubles in the first 100 cycles.

Regarding the heat transfer rates, it was found that both convection and radiation had an unimpressive importance over the course of aging. The thermal conduction heat transfer rate is the major contributor to the thermal energy dissipation of the cell, and its slope, as well as that of the heat generation rate, followed the trend of the reduction ohmic resistance over the cycles. It was also verified that the addition of the reversible heat term did not cause a significant change in the estimated internal temperature of the cell, definitely indicating that entropy coefficient is not relevant in this case. Comparing the preset work with the method used by Tripathy *et al.* (2017), it is clear that the heat generated due to R_0 as function of number of cycles is much more relevant than the parcel due to differential voltage.

5. REFERENCES

Bergman, T. L., Lavine, A. S., Incropera, F. P. and Dewitt, D. P., 2014 *Fundamentals of heat and mass transfer*. John Wiley & Sons, Hoboken-NJ, seventh edition

Bernardi, D., Pawlikowski, E., Newman, J., 1985. "A general energy balance for a battery system". *Journal of the Electrochemical Society: Eletrochemical Science and Technology*, Vol.132, pp. 5-12.

Churchill, S.W., e Burnstein, J., 1977. Heat Transfer.99.300.

Dong, T., Peng, P. and Jiang, F., 2018. "Numerical modeling and analysis of the thermal behavior of NCM lithium-ion batteries subjected to very high C-rate discharge/charge operations". *International Journal of Heat and Mass Transfer*, Vol. 117, pp. 261-277.

Forgez,C., Doa, D.V., Friedricha, G., Morcrette, M., Delacourtb, C., 2010. "Thermal modeling of a cylindrical LiFePO4/graphite lithium-ion battery". *Journal of Power Sources*, Vol. 195, pp. 2961-2968

Nazari, A. and Farhad, S., 2017. "Heal generation in lithium-ion batteries with different nominal capacities and chemistries". *Applied Thermal Engineering*, Vol. 125, pp. 1501-1517.

Nadimpalli, S., Abraham, D.P., 2015 "Stress evolution in lithium-ion composite electrodes during electrochemical cycling and resulting internal pressures on the cell casing". *Journal of the Electrochemical Society*, Vol.162, pp. A2656-A2663.

Samba, A., 2015. "Battery electrical vehicle analysis of thermal modeling and thermal management". *WMG,Université de Caen Basse Normandie*, Caen, France.

Shuai, M., Modi, J., Tao, P., Song, C., Wu, J., Wang, J., Deng, T. and Shang, W., 2017. "Temperature effect and thermal impact in lithium-ion batteries: A review". *Progress in natural science: materials international*, Vol. 28, pp. 653-666.

Tripathy, Y.,McGorgon, A., Low, J. and Marco, J., 2017. "Internal temperature prediction of lithium-ion cell using differential voltage technique". *WMG, University of Warwick, Coventry*, United Kingdom.

USABC Battery Test Procedures Manual., 1996. "Electric vehicle battery test procedures manual", Review 02.

Waldmann, T., Wohlfahrt-Mehrens, M., 2015. "In-operando measurements of temperatures gradients in cylindrical lithium-ion cells during high-currents discharge". *ESC Electrochemistry Letters*, Vol. 4, pp. A1-A3

Wang, S., 2016. "Entropy and heat generation of lithium cells/batteries". *Chinese Physical B* , Vol. 25

Wang, Z., Ma, J. and Zhang, L., 2017. "Finite element thermal model and simulation for a cylindrical li-ion battery". *Special sectionon battery energy storage and management system*.

Zografos, A.I., Martin, W.A, Sunderland, E., 1987. "Equations of properties as a function of temperature for seven fluids". Computer Methods in Applied Mechanics and Engineering , Vol. 61, pp. 177-187.

6. RESPONSIBILITY NOTICE

The authors are the only responsible for the printed material included in this paper.